International Journal of Mass Spectrometry 223–224 (2003) 507–518

www.elsevier.com/locate/ijms

Proton transfer reaction mass spectrometry at high drift tube pressure

D.R. Hanson*, J. Greenberg, B.E. Henry, E. Kosciuch

Atmospheric Chemistry Division, National Center for Atmospheric Research, Boulder, CO, USA

Received 2 January 2002; accepted 5 June 2002

Abstract

An ion drift tube operated at a total pressure of 10 Torr (∼13 mbar) coupled to a mass spectrometer is described. Proton transfer from water molecules was used to detect organic compounds and calibrations of the instrument yield normalized sensitivities that are in accord with what is expected for operation at this pressure. For example, the sensitivity for acetone was found to be 240 Hz ppbv^{-1} for 1 MHz of reagent ion signal while that for isoprene was 120 Hz ppbv^{-1}. Issues particular to using this technique at pressures of 10 Torr, considerably higher than the conventional pressure, are addressed. Detection limits for a 1 s integration ($S/N = 2$) depend on the cleanliness history of the system but can reach as low as 20 pptv. (Int J Mass Spectrom 223–224 (2003) 507–518)

Keywords: Proton transfer reaction mass spectrometry; Drift tube pressure

1. Introduction

Werner Lindinger's pioneering work on the detection of volatile organic compounds via proton transfer from water molecules has opened up a new area of application for mass spectrometry. The instruments that Lindinger and co-workers [1–3] have developed have already made large impacts on the fields of analytical chemistry and atmospheric chemistry. Proton transfer mass spectrometry has contributed to the study of atmospheric chemistry both in the laboratory and in field applications. It has become a very useful tool when a fast response sensor is needed. A few examples are: leaf-wound compound investigations [4–6], laboratory heterogeneous chemistry [7], trace gas monitoring [1,8], and flux measurements [9].

We have followed their lead by developing an ion drift tube that can operate at a pressure of ∼10 Torr. Sensitivity usually increases with pressure and the sensitivity scales linearly with pressure for a given reagent ion intensity and ion-molecule reaction (drift) time. Also, at these pressures ionization via alpha particles is sufficient that low-level radioactive sources can be employed. This type of ion source produces very few radicals and may provide relatively clean background conditions. Here we describe a new instrument, designed and constructed in-house, that is currently being used to monitor volatile organic compounds (VOCs) in laboratory experiments.

2. Experimental

The ion source and drift tube, both at 10 Torr pressure, are coupled to a differentially pumped

* Corresponding author. E-mail: dhanson@ucar.edu

1387-3806/02/$ – see front matter
PII S1387-3806(02)00924-7

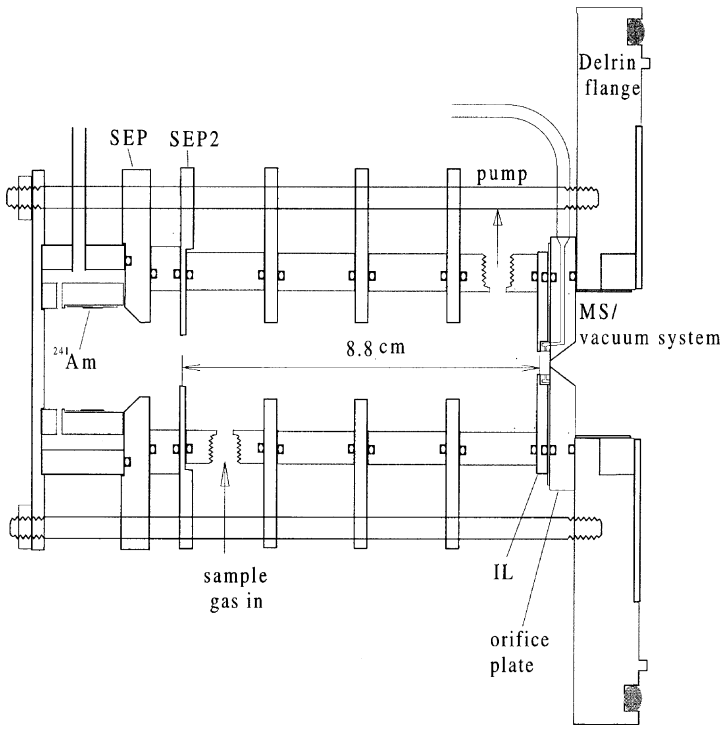

Fig. 1. Cross-sectional drawing of ion source, source exit plates (SEP and SEP2), drift region (between SEP2 and IL, ~8.8 cm), and mass spectrometer inlet region (IL and orifice plate). They are mounted on a plastic flange that is connected to an MS/high vacuum system. To prevent static charge buildup, portions of the plastic that might incur a charge and affect the path of the ions in the vacuum system are covered by conducting material (steel).

quadrupole mass spectrometer. The ion source and drift tube are depicted schematically in Fig. 1. The differentially pumped vacuum and quadrupole systems are typical of similar chemical ionization mass spectrometers (e.g., the two highest vacuum stages of Huey et al. [10] and Neuman et al. [11]). Two separate vacuum systems/quadrupole mass spectrometers have been constructed and several similar drift tubes have been tested and mainly one design is described. The dilution system for performing calibrations is also described.

2.1. Ion source

The ion source is a radioactive strip of ^{241}Am (~1.2 mCi, standard film, NRD Incorporated, Grand Island, NY) rolled up inside a stainless steel cylinder (2.65 cm i.d. by 1.4 cm long). This amount of activity yields about $\sim 10^7$ alpha particles s^{-1} impinging on the gas inside the source. Assuming an ionization efficiency of 400 ion pairs cm^{-1} of travel at 10 Torr [12], 2 cm of travel on average, the total ion production rate is $\sim 10^{10}$ s^{-1} in the ion source. Supposing 20% of these are extracted and sent into the drift tube, the total ion current through the gas in the drift tube would be ~300 pA. This order-of-magnitude estimate is in accord with measurements of the current on the orifice plate that ranged from 300 to 900 pA. A flow of nitrogen (5–20 sccm) and water vapor (~0.2–1 sccm) minimizes the back diffusion of analyte gases into the source. The formation of O_2^+ and other background ions are thereby suppressed; e.g., the signal at 32 amu is typically 0.02% or less of the water proton cluster signals. The ion source is held at a high positive potential; for a 10 cm drift tube length, it is typically in the range of 2.5–5 kV.

The ion source and drift tubes have been coupled in several different ways. There is generally a region separated by two stainless steel disks 0.6–1.9 cm apart with 1–1.8 cm i.d. holes. The plate closest to the source (source exit plate (SEP)) is in contact with the source and is thus at the same potential. When a second plate was present (SEP2), the potential difference between it and SEP was chosen to give an electric field that matched or exceeded the electric field in the drift tube. In this way, higher water clusters were transformed into $H_3O^+H_2O$ and possibly H_3O^+ before they came into contact with the sample gas in the drift tube. These plates also cut off line-of-sight alpha particles from entering the drift tube eliminating the formation of ions in the drift region.

2.2. Drift tube

The drift tube, typically 8–10 cm in length, is constructed of circular stainless steel guide plates (0.3 cm thick by 1.9 cm i.d.) that are separated by static dissipative (SD) teflon cylinders (1.9 cm length by 3.5 cm i.d.) This material has a volume resistivity of $\sim 10^{11}$ ohm cm (Semitron ESD 500, Quadrant Engineering Plastics). Viton o-rings provide seals between the SD teflon and guide plates and fittings. Four threaded nylon rods hold the drift tube and source to the mass spectrometer flange. A flow (typically 85 sccm) of sample gas is sent into the drift tube transverse to the ion velocity. This flow is set via a critical orifice ($\sim$110 μ diameter for sampling at 610 Torr). Alternatively, to check for background count rates, clean, dry nitrogen or air is sent to the drift tube. These flows enter the drift tube near its top and exit it near the bottom. The average residence time for the sample gas is 0.7 s.

The gas flow exits the drift tube through a port near the mass spectrometer inlet. A regulating valve before the pump (the backing pump for the vacuum system) is adjusted to maintain the desired pressure in the drift tube. Some of the flow, about 5 sccm, enters the high vacuum/MS system along with a fraction of the ions. The inlet to the mass spectrometer consists of two plates with holes for ions and gas to pass through that are $\sim$0.34 cm apart (between midpoints.) The 0.15 cm thick first plate (inlet lens (IL)) has a 0.5 cm i.d. hole and the second (orifice plate) has a $\sim$200 μm aperture (a 0.95 cm diameter, 50 μm thick, stainless steel disk, Lenox Laser, Glen Arm, MD.) A small SD teflon cylinder presses the aperture disk against an o-ring to provide a seal to the vacuum system. The IL plate and the orifice plate are electrically separated by a 0.05 cm thick teflon disk (sealed with o-rings) so that a potential difference can be applied between them. The electric field in the inlet region in front of the orifice is usually set to match the electric field in the drift tube. This electric field can be increased to induce dehydration of ions if desired. A flow of dry gas can be introduced between these plates that will lead to additional drying of the ions as well as to less H_2O vapor entering the mass spectrometer.

An electrostatics computer program (Simion 3D, Bechtel BWXT, Idaho) was used to calculate the electrostatic potential within the source region and the drift tube. Fig. 2 depicts a two-dimensional slice of this region where the lens plates, equipotential lines, and ion paths are shown. The static dissipative material was assumed not to disturb the electric field. An average electric field was calculated from the applied potentials divided by the distances between the midpoints of the lenses. Along the axis of the drift region, the electric fields were within 7% of the calculated average electric field for 90% of the drift tube length. The electric field deviated most from the average electric field near the entrance and the exits of the drift tube. The electric field at the midpoint of SEP was about 50% of the average field but in the first 0.5 cm quickly rose to the average value. At the end of the drift tube near the midpoint of the LI plate, the ions experience a $\sim$20% decrease in the electric field. The field increases as the ions travel toward the orifice and at a distance of 0.15–0.2 cm before the ions enter vacuum, the electric field increases to a value about 10% greater than the average field.

The paths for the ions were calculated by including a drag factor on the ions. The drag factor simulates collisions of the ions with the bath gas so that a specified drift velocity is obtained. One can see that ions from the source are focused into a beam with a rather

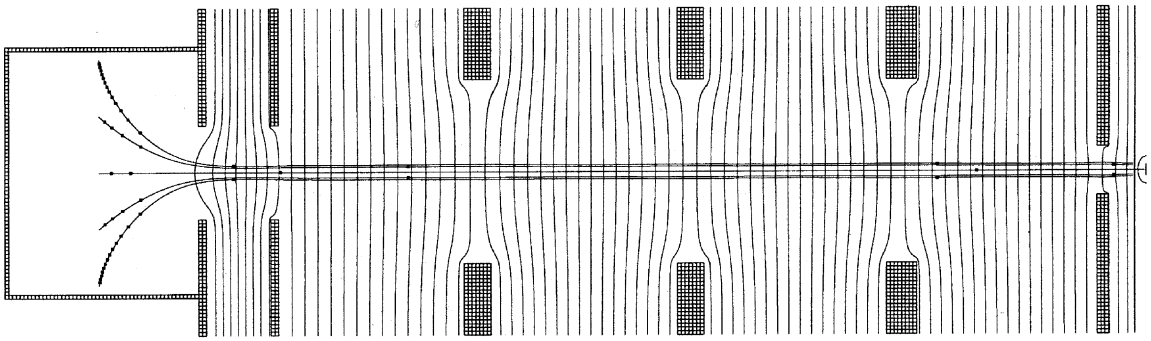

Fig. 2. Cross-section of the ion source, drift region, and inlet regions. Lens plates, calculated electrostatic potential lines (50-V intervals), and sample ion paths (dots along a path indicate 100-μs intervals) are depicted. See text for further details.

narrow diameter (~0.14 cm in Fig. 2). The diameter of the beam was fairly independent of axial position within the source. A narrow diameter ion beam is consistent with our observation that the total ion signal depends strongly on the alignment of the drift tube parts. Slight misalignment of the source region or lens plates, of the order of 1 mm or so over the length of the drift tube, noticeable by holding a straight edge along the edges of the plates, lead to large decreases (80% or more) in reagent ion count rates.

Along the ion paths are markers that are separated by 100-μs drift time intervals. Note that space charge effects were not included in the simulation. These effects would be expected to affect the paths of ions that are moving rather slowly, i.e., those ions in the source that are created far off axis. Also, in regions of weak fields where the ions move slowly, ion-pair recombination is likely to occur with a greater efficiency than in regions with strong fields. Thus, although the simulation indicates that a majority of the ions created within the source can be extracted and focused into the drift region, it is probable that the ions that enter the drift region are generated primarily in a cylindrical volume within the source that has a diameter close to that of the source exit plate.

Drift tubes similar to that shown in Fig. 1 have been employed to detect VOCs using proton transfer and to better understand the level of hydration (distribution) of water–proton clusters and their ion chemistry. In a laboratory study on the solubility of nopinone [7], the drift tube consisted of a 10 cm long by 3.5 cm i.d. tube of SD teflon. Reagent ion count rates were high (up to 5 MHz) and sensitivities were adequate for many VOCs; however, some ions (e.g., protonated benzene) experienced unexpected breakup. This was probably due to large non-uniformities in the field in the drift region (there were no guide rings inside the drift tube). A drift apparatus has been constructed where the drift region closely approximates the gap between two large plates. Fig. 3 depicts a cross-section of the radioactive source, lens, and mass spectrometer inlet. These

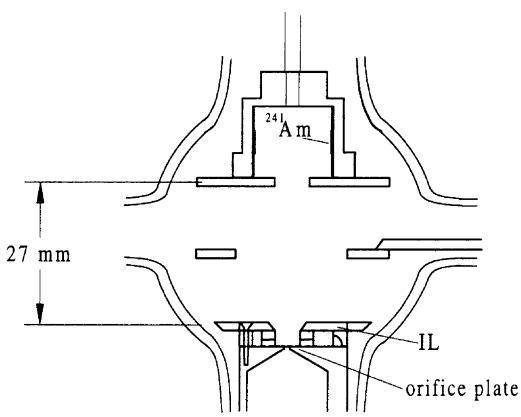

Fig. 3. Cross-section of alternate drift apparatus showing ion source, drift region with one guide lens, and mass spectrometer inlet region. The drift region is enclosed in a glass tube (5 cm i.d.); there is a flow of 360 sccm N_2 perpendicular to the page. The guide ring prevents static charge on glass enclosure from affecting the path of the ions. Distance between ion source and IL is 2.69 cm.

are mounted transverse to the axis of a 5 cm i.d. glass flow tube. A large flow of dry N_2 (360 sccm) was flowed across the path of the ions. A small flow of N_2 (10 sccm) and H_2O (0.5 sccm) through the source is diluted by this flow. Because there was essentially no distance allowed for these flows to mix, the pH_2O along the majority of the ion path is probably much less than that calculated assuming full mixing of the humidified source flow (0.015 Torr.) This drift apparatus was used to study the rate of conversion of $H_3O^+H_2O$ to H_3O^+ as a function of electric field.

2.3. Ion velocities and instrument sensitivity

With a typical electric field E of 350 V cm^{-1} at 10 Torr, the field strength $E/N = F_s$ is ~108 Td. The drift velocity v_d of an ion with reduced mobility $\mu_o = (P/760\,\text{Torr})(273\,\text{K}/T)\mu$ is given by

$$v_d = E\mu = \frac{E}{P}\left(\frac{760T}{273}\right)\mu_o = 268\mu_o F_s \quad (1)$$

where the last expression is valid for 298 K assuming μ_o does not depend on v_d. μ_o for H_3O^+ and $H_3O^+H_2O$ are 2.8 and 2.4 cm^2 V^{-1} s^{-1}, respectively [13]. For these conditions, H_3O^+ has a v_d of 8×10^4 cm s^{-1} and the ion residence time is 120 μs for a 10 cm long drift region. For low analyte mixing ratios (<300 ppbv), the theoretical detection sensitivity of the instrument S_t is given by

$$S_t = Rktf(3.24 \times 10^8) \quad (\text{Hz ppbv}^{-1}) \quad (2)$$

where R is the reagent ion count rate, k the ion-molecule reaction rate, and t is the ion drift time. The last two factors are a dilution factor f (due to the flow through the source; typically equal to 80/100) and the concentration of a trace analyte gas at a mixing ratio of 1 ppbv at a total pressure of 10 Torr and temperature of 298 K. For nominal conditions $R = 1$ MHz, $k = 3 \times 10^{-9}$ cm^3 s^{-1}, and $t = 10^{-4}$ s, the sensitivity of the instrument would be ~80 Hz ppbv^{-1}.

Eq. (1) is based on the simplification that the reaction rate coefficients of the analyte with H_3O^+, $H_3O^+H_2O$, etc., are similar. Because this is not true for some species, Hansel and co-workers [2] have designed their ion source such that mostly H_3O^+ ions enter the drift tube. Thus, fairly accurate theoretical sensitivities can be calculated. Using the theoretical sensitivities to calculate trace gas concentrations requires knowledge of mass-dependent detection efficiencies (i.e., mass discrimination) that can be determined experimentally. Because R can be variable, Warneke et al. [14] have introduced the concept of normalized counts per second (ncps) so that different instruments and calibrations can be compared. For (2), R is set to 1 MHz and for a calibration of an instrument, the analyte count rate is normalized to 1 MHz reagent count rate (i.e., multiplied by the ratio 1 MHz/R). We will designate this sensitivity as S_t.

The electric field in a clean drift tube can be maintained at a strength as high as ~170 Td (500 V cm^{-1} at 10 Torr) without a discharge occurring. If it has been exposed to high concentrations (>300 ppbv) of organic compounds for long periods of time, this threshold voltage has been seen to decrease. The drift tube pieces are periodically cleaned ultrasonically in a dilute soap solution followed by thorough rinsing and drying.

2.4. Mass spectrometer

When the drift tube is at 10 Torr, a 200 μm entrance aperture gives a gas flow of ~5 sccm into the vacuum system. The number of reagent ions entering the vacuum system can be roughly estimated from the flux of ions in the inlet region. The current from the ion source, estimated above to be ~300 pA or 2×10^9 ions s^{-1}, if spread over a circle of 0.15 cm in diameter, would result in a flux of 10^{11} ions cm^{-2} s^{-1}. This value for the ion flux is reasonable as it is consistent with an ion density of 10^6 cm^{-3} moving at a drift velocity of 8×10^4 cm s^{-1} (the flux of ions is the product of the ion density times v_d). Multiplying this flux by the area of the orifice yields a value of ~4×10^7 ions s^{-1} entering the vacuum system. If the overall ion transmission and detection efficiency of the mass spectrometer is 5–10%, a total ion count rate of ~2–4 MHz would be expected. The observed count rates for the sum of H_3O^+ and $H_3O^+H_2O$ for this size aperture are typically 2–3 MHz. Consequently, it appears that the ions stay in a somewhat tight grouping

as they move along the drift tube. A small spreading of the ion beam is consistent with space charge effects being negligible compared to the applied electric field in the drift tube; this is expected to be the case for ion concentrations $\leq 10^6\,cm^{-3}$ [15].

The inlet is attached to the vacuum system on a flange made of Delrin (shown in Fig. 1) so that the aperture can be readily floated at a potential above ground. On the vacuum side of the flange is attached a stainless steel disk (12 cm o.d. with a 3.8 cm hole) so that ions are not exposed to the flange material. In addition, a small stainless steel cylinder surrounds the ion beam as it passes through a 3.68 cm hole in the plastic. Between them to cover any exposed plastic is a ring of SD teflon. The stainless steel parts also serve as lenses for focusing ions in the system.

The mass spectrometer is differentially pumped with ~650 L s^{-1} pumping speed on the front chamber and 220 L s^{-1} on the back chamber (Varian Vacuum, Lexington, MA). The front chamber has a series of ion lenses through which the ions are focused the last of which has a 1.3 cm opening to the back chamber (quadrupole entrance lens). With these pumping speeds and an inlet flow of 5 sccm, the front and back chamber pressures are calculated to be $\sim 1 \times 10^{-4}$ and 5×10^{-6} Torr, respectively. We have operated the system at pressures up to four times these values without any significant decreases in the performance of the instrument. The quadrupole (rod diameter of 1.905 cm, length 22.2 cm), channel electron multiplier, and preamplifier are located in the back chamber. The multiplier is operated in pulse counting mode and the multiplier–preamplifier combination has a maximum count rate of ~1 MHz. The reagent ions, usually H_3O^+ or $H_3O^+H_2O$ (19 and 37 amu, respectively), can have count rates that substantially exceed 1 MHz; thus, their isotopic species (21, 38, or 39 amu) are generally monitored to provide a measure of the signals due to H_3O^+ and $H_3O^+H_2O$.

2.5. Dilution system and supplies

A dilution system based on successive dilutions of a standard gas containing analytes at 3–10 ppmv mixing ratios was used to prepare a flow of gas with analytes present at low ppbv levels. This flow was introduced into the instrument to provide a calibration of the detection sensitivity. One gas cylinder contained methanol, acetaldehyde, acetone, isoprene, methylbutenol (2,3,2), and α-pinene. Another standard contained only isoprene. The concentrations of analytes in the standard mixture were known by their gravimetric preparation and all the species were periodically checked with a gas chromatograph system for changes over time. The relative humidity (RH) of the sample gas is controlled at the last stage of dilution by setting the relative flows of fully humidified gas and of dry gas.

Nitrogen was taken from either the gas over liquid nitrogen or an UHP grade cylinder. High purity air was taken from a zero air generator (Adco, Clearwater, FL); this air was in addition passed over a home-made catalytic converter (Pt on alumina at 300 °C). Liquid water was taken from either deionized and/or distilled water. Generally, the liquid water was purged with nitrogen gas (a flow of nitrogen was bubbled through it for several hours) yielding a sample of water that evolved dissolved gases at a concentration no greater than the sample gas in the instrument. The water introduced into the ion source was taken from the vapor pressure over liquid water (~20 Torr) and metered with a leak valve. The mass flow rate of water from this leak valve was calibrated by monitoring the level of liquid water in the reservoir or by measuring the water content of the exhaust of the drift tube (frost point sensor, EdgeTech, Milford, MA).

3. Results and discussion

3.1. Water–proton cluster distributions

The equilibrium constants for the reactions

$$H_3O^+ + H_2O \leftrightarrow H_3O^+H_2O \quad (3a)$$

$$H_3O^+H_2O + H_2O \leftrightarrow H_3O^+(H_2O)_2 \quad (3b)$$

$$H_3O^+(H_2O)_{n-1} + H_2O \leftrightarrow H_3O^+(H_2O)_n \quad (3c)$$

have been measured by Lau et al. [16] and Cunningham et al. [17] for clusters up to $n = 5$. Their measurements were performed in heated chambers and the ions, water molecules, and bath gas were at the same temperature. A kinetic temperature T_{eff} for an ion moving at v_{d} can be calculated [18] according to

$$T_{\text{eff}} = T_{\text{r}} + \frac{Mv_{\text{d}}^2}{3k} \tag{4}$$

where T_{r} is the temperature of the bath gas, M the mass of the bath gas, and k is the Boltzman constant. Note that the energy deposited into the bath gas via collisions with ions is very small compared to the bath gas thermal energy. Thus, T_{r} can be taken to be the temperature of the drift tube wall. This temperature can be used along with the equilibrium constants of Lau et al. to obtain estimates of the ratios of successive ions.

These ratios likely only serve as rough guides for setting experimental conditions as true thermodynamic equilibrium might not be expected in a drift tube. Also, the lifetime for decomposition of a cluster might be comparable to, or longer than, the drift time. The clusters $H_3O^+(H_2O)_n$ drift at a given velocity resulting in a T_{eff} (up to 1200 K) that is much greater than the temperature of the bath gas and water molecules, T_{r}. This situation is evidently different than that for the experimental investigations of Lau et al.

We found that the electric field strength needed to have primarily the H_3O^+ ion present (125 Td) was somewhat larger than what would be predicted by applying the Lau et al. thermodynamics (105 Td) along with (4) to our experimental conditions (water partial pressure, pH_2O, ranging up to 0.35 Torr). This may be because the collision of $H_3O^+H_2O$ with an N_2 molecule (rotationally and vibrationally cold) may not lead to decomposition whereas it would if N_2 was thermalized at the temperature T_{eff}. Even though the kinetic energy of the collision is large, some of the energy can go into exciting rotational and vibrational modes of the N_2 collision partner (also see the discussion in Ellis et al. [18]). Thus, lifetimes for 37 amu ions longer than those found by Lau et al. might be expected.

We measured the approximate lifetimes of $H_3O^+H_2O$ using the apparatus shown in Fig. 3. The electrostatics of this arrangement was also evaluated. In the 2.69 cm drift region, the electric field was constant (to within 5%) over about 2 cm. In the mass spectrometer inlet section, the electric field was highest and relatively constant (variations <5%) over the last ~0.2 cm before the ions entered the MS vacuum system. For an $E = 325\,\text{V cm}^{-1}$, the drift times, calculated from drift length divided by v_{d} from (1), are approximately 30 and 3 μs in the two regions, respectively. By increasing the electric field in the inlet section and observing the change in the ratio of 37 amu to 19 amu, we can arrive at an estimate of the lifetime of $H_3O^+H_2O$ as a function of electric field. Furthermore, we can use the combined drift times of these two regions and the measured 37 amu to 19 amu ratio to get an estimate of the lifetime at an $E = 325\,\text{V cm}^{-1}$. In this case, we assume that the ions exiting the source are 37 amu or larger and that the larger hydrates are quickly converted to 37 amu.

One such experiment is shown in Fig. 4 which is a plot of the fraction of the total ion signal for 19, 37, and 55 amu vs. E in the inlet region for H_3O^+ and $H_3O^+H_2O$. The drift tube region electric field was $E = 325\,\text{V cm}^{-1}$. The N_2 pressure was 10.0 Torr. During the inlet region drift time of 2 μs, an ion experiences thousands of collisions. Supposing that the $[H_3O^+H_2O]$ to $[H_3O^+]$ ratio is altered only by the decay of $[H_3O^+H_2O]$ in the time dt it spends in the inlet region, the lifetime of $H_3O^+H_2O$, $\tau_{37}(E)$, can be obtained from

$$\tau_{37}(E) = -\frac{\text{d}t}{\ln\{[37\text{a}](\text{d}t)/[37\text{a}](0)\}} \tag{5}$$

where $\text{d}t = l/v_{\text{d}}$, $l = 0.2$ cm, v_{d} is taken from (1) and is a function of E, and [37a](dt) is the ratio of the signal at 37 amu to the total ion signal at time dt. The value of [37a](0) is taken to be that when E is equal to the electric field in the drift region ($325\,\text{V cm}^{-1}$). For a variation of E from 450 to $350\,\text{V cm}^{-1}$, dt varies from 2.2 to 2.9 μs. A lifetime at $325\,\text{V cm}^{-1}$ was obtained using $\text{d}t = 34$ ms (i.e., including the time in the drift region) and assuming [37a](0) = 1. The

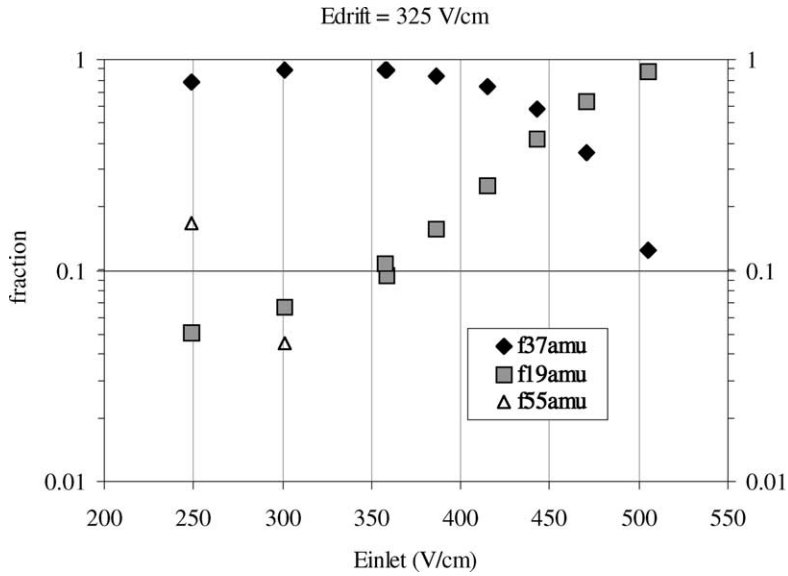

Fig. 4. Fraction of ions at 19, 37, and 55 amu as a function of electric field in the mass spectrometer inlet region (between IL and orifice plate, see Fig. 3).

resulting lifetimes for $H_3O^+H_2O$ are 470, 110, 17, and 3.6 μs for E = 325, 350, 400, and 450 V cm^{-1}, respectively. This is a very strong dependence on electric field, i.e., an 8% increase in E results in a 75% decrease in τ_{37}. These results indicate that to obtain primarily H_3O^+ reagent ions in a time shorter than the typical drift time of 100 μs, the electric field at 10 Torr total pressure should be 400 V cm^{-1} or greater ($F_s \geq 123$ Td).

The lifetime of $H_3O^+H_2O$ at 806 K (F_s = 104 Td, E of 337 V cm^{-1} at 10 Torr, Eqs. (1) and (4)) reported by Cunningham et al. [17] is 53 μs. This value was obtained in CH_4 at a number density of 4.8×10^{16} cm^{-3}. Supposing the reaction is at the low pressure limit [16,17,19] at 10 Torr of N_2 (number density of 3.24×10^{17} multiplied by the ratios of the Langevin cross-sections of 0.69 [16]), the lifetime of $H_3O^+H_2O$ should be 10 μs. The lifetime of $H_3O^+H_2O$ at this electric field, interpolated from the measurements presented here, is about 200 μs or roughly an order of magnitude longer than that predicted from the Cunningham et al. data. This is evidence that the effectiveness of the collisions in the drift tube is less than if the bath gas was also heated. In other words, the internal energy of a molecular ion is characterized by a temperature T_{int} which may be quite different than T_{eff} [18].

The RH of air sampled at atmospheric pressure may lead to concentrations of H_2O up to 10^{16} cm^{-3} at a drift tube pressure of 10 Torr, much higher than for a drift tube operated at 2 Torr total pressure. Therefore, the forward rate for (3a) may become large enough that significant conversion of H_3O^+ ions to $H_3O^+H_2O$ ions occurs. At the low pressure limit the increase in forward rate with total pressure is quadratic (the number density of H_2O scales with pressure for a given sample gas RH). If the rate for (3a) is at the low pressure limit for number densities up to 3.24×10^{17} cm^{-3} [17,19], then the conversion of H_3O^+ to $H_3O^+H_2O$ could be very fast. A psuedo-first-order conversion time at 806 K is given by [17] $\{(7 \times 10^{-29}\ \text{cm}^6\ \text{s}^{-1}) \times 0.69 \times (3.24 \times 1017\ \text{cm}^{-3}) \times (1016\ \text{cm}^{-3})\}^{-1} = 6$ μs at 10 Torr N_2 and 3% H_2O. Therefore, a high E/N may be more important at 10 Torr than at 2 Torr to maintain mostly H_3O^+ ions in the drift tube.

The water mixing ratio of a sample gas can be as high as 3.3% (100% RH at 298 K and 610 Torr) resulting in numerous collisions of $H_3O^+(H_2O)_n$ ions

with H_2O molecules. In this case, processes such as resonant charge transfer (A. Hansel, private communication) may play a role in determining the abundance of the $H_3O^+(H_2O)_n$ ions.

3.2. Calibrations

Shown in Fig. 5 are the sensitivities S_t, S_t normalized to 1 MHz, for methanol, acetaldehyde, acetone, isoprene + methylbutenol, and α-pinene as a function of RH of the sample gas. The flow of water in the source once it enters the drift tube is equivalent to ~20% RH in the sample flow. The electric field was 370 V cm^{-1} and pressure was 10.0 Torr ($F_s = 114$ Td) and the drift tube had a length of 8.8 cm. This yields a reaction time of 100 μs for H_3O^+ and 115 μs for $H_3O^+H_2O$ if it drifts independently of H_3O^+. At low RH, the reagent ions were ~70% H_3O^+, 27% $H_3O^+H_2O$, and 3% $H_3O^+(H_2O)_2$. At the highest RH they were measured to be 50% H_3O^+, 38% $H_3O^+H_2O$, and ~12% $H_3O^+(H_2O)_2$. These serve only as rough guides as it is not known how much these ratios are altered when the ions are sampled into the vacuum system.

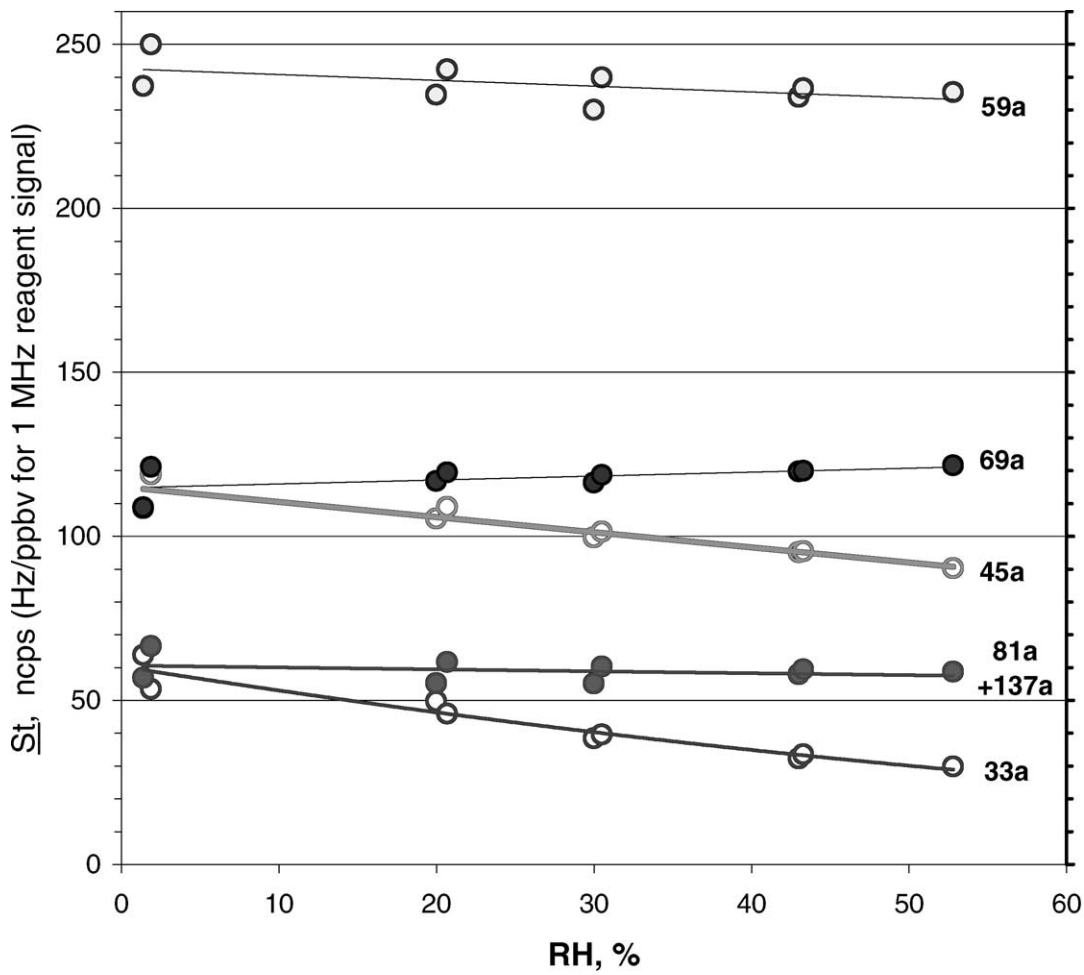

Fig. 5. Normalized sensitivities of the instrument for acetone (59 amu), isoprene + methylbutenol (69 amu), acetaldehyde (45 amu), α-pinene (81 and 137 amu), and methanol (33 amu). Total pressure was 10.0 Torr and $E = 370$ V cm^{-1}.

The S_t for acetone of 240 Hz ppbv^{-1} for 1 MHz of reagent ion signal is independent of RH. The average sensitivities S_t for isoprene and methylbutenol, 120 Hz ppbv^{-1} (methylbutenol appears almost exclusively at 69 amu as it easily loses an H_2O molecule for these conditions), and that for α-pinene, 60 Hz ppbv^{-1}, are also independent of RH. On the other hand, the S_t for acetaldehyde (115–90 Hz ppbv^{-1}) and for methanol (60–30 Hz ppbv^{-1}) depend on RH indicating that the back reaction

$$H^+ \cdot VOC + H_2O \rightarrow H_3O^+ + VOC \quad (6)$$

may be occurring at a significant rate in our system at high RH. The heat of reaction for (6) for methanol is about 14 kcal mol^{-1} and that for acetaldehyde is 16 kcal mol^{-1} (NIST Chemistry Web Book). These are the least endothermic of the analytes presented here. Hansel et al. [20] investigated the sensitivity of proton transfer reaction mass spectrometry (PTR-MS) towards formaldehyde (5 kcal mol^{-1} for (6)) and demonstrated a large influence of the back reaction on the sensitivity. At the elevated water concentrations present at the higher pressures here (approximately a factor of five with respect to the systems of Lindinger et al. and others [8]), back reactions might be expected to reduce the sensitivity of instrument for methanol and acetaldehyde. Note that the possible interference of $CH_3OH{\cdot}H^+{\cdot}(H_2O)_2$ in the detection of isoprene and MBO at mass 69 was negligible. This was based on the observation that only small amounts of $CH_3OH{\cdot}H^+{\cdot}H_2O$ (51 amu; signal was ∼10% or less of the signal for $CH_3OH{\cdot}H^+$) were present for these conditions.

Shown in Table 1 are the measured sensitivities presented earlier and those of Warneke et al. [14] and de Gouw et al. [5] for E/N of ∼110 Td. The drift tube parameters are also listed. Taking into account drift time differences (8.8 cm vs. 10 cm drift regions) and our dilution factor f (a factor of ∼85/105), our S_t at 10 Torr should be 3.5–4 times that of Warneke et al. As can be seen by comparing the values in Table 1, our sensitivities for acetaldehyde, acetone, and isoprene are about 3.5, 2, and 3 times, respectively, those of Warneke et al. These factors are on average somewhat lower than the expected factor of 3.5–4. The experimental conditions reported by de Gouw et al. ranged from 1 to 2 Torr pressure and E = 35–70 V cm^{-1} (the midpoints of these ranges are used here; 1.5 Torr and E = 52.5 V cm^{-1}) and the drift region was 49 cm long. Combining these factors together, our S_t and that of de Gouw et al. should be about the same. Note that the calibration factors of de Gouw et al. were reported for a reagent ion signal of 5×10^5 Hz, and thus were multiplied by a factor of two in Table 1. The S_t from these instruments compare favorably well with our instrument on average having a slightly higher sensitivity than that of de Gouw et al.

We observed that S_t depended upon the settings of some of the ion lenses as well as the mass resolution of the instrument (typical resolution $M/\Delta M$ was 100).

Table 1
Comparison of experimental conditions and calibration factors (at E/N ∼ 110 Td) for similar instruments

Analyte	Experimental condition		
	S_t (this work)[a]	S_t (Warneke et al.)[b]	S_t (de Gouw et al.)[c]
	Pressure (Torr)		
	10	1.88	1.5[c]
	Drift region length (cm)		
	8.8	10	49
Methanol	60–30[d]	–	30
Acetaldehyde	115–90[d]	35	110
Acetone	240	130	156
Isoprene	120[e]	42	–
α-Pinene	60	–	36

[a] Normalized sensitivity (Hz ppbv^{-1} MHz^{-1} of reagent ion) and E = 370 V cm^{-1}; accuracy of concentrations in standard gas is estimated to be ±25% (±40% for methanol and acetaldehyde).

[b] S_t reported by Warneke et al. [14]; P = 1.88 Torr and E = 65 V cm^{-1}.

[c] S_t calculated from calibration factor reported by de Gouw et al. [5] for 0.5 MHz of reagent signal; average of reported conditions: P = 1.5 Torr and E = 52.5 V cm^{-1}.

[d] Values dependent upon RH of sample flow; S_t decreased as RH increased.

[e] This value was taken from Fig. 5 and is the average of the S_t for methylbutenol and isoprene. It is consistent with values obtained in experiments where methylbutenol was not present.

These were set to maximize the overall signal with only cursory attention paid to minimizing variations with mass, thus mass discrimination effects were not fully evaluated. This may contribute significantly to the sensitivity of our instrument to a particular compound and may be part of the reason for the variations presented earlier. A higher proportion of $H_3O^+H_2O$ in our drift region might also contribute. Uncertainties in the standard gas concentrations must also be considered. A more accurate comparison of the sensitivities among instruments would require detailed information on the various factors listed here; we did not investigate these factors thoroughly nor is this information included in the literature cited. Nevertheless, the sensitivities for these species increase with pressure roughly in accord with expectations.

3.3. Detection limits

With a typical reagent ion signal of 3 MHz, the sensitivity of the instrument for acetone and isoprene is 720 and 350 Hz ppbv^{-1}, respectively. With half the signal for α-pinene appearing on 137 amu, the sensitivity for this species is about 100 Hz ppbv^{-1}. With nominal background signals of 200, 10, and 5 Hz at 59, 69, and 137 amu, respectively, the 1-s detection limits (signal/noise = 2) for acetone, isoprene, and α-pinene are 40, 20, and 45 pptv, respectively. The background signal levels depend on the history of the instrument and are variable, however, many regions of the mass spectrum are typically very clean with background signals of 10 Hz or less. Therefore, 1-s detection limits of 20 pptv or better might be expected for many compounds.

Clustering of reagent ions with N_2 was observed to occur. The signals at 47 and 75 amu due to $N_2{\cdot}H_3O^+$ and $(N_2)_2{\cdot}H_3O^+$ were typically 1 and 0.2%, respectively, of the signal for H_3O^+. These ions were presumably due to clustering processes occurring during the expansion into the vacuum system. These ions and others like them (e.g., $N_2{\cdot}H_2O{\cdot}H_3O^+$) would limit the detection sensitivity of the instrument for compounds that appear at those masses. To decrease these possible interferences, a collision dissociation chamber could be added to de-cluster weakly bound ions such as $N_2{\cdot}H_3O^+$.

4. Summary

A proton transfer mass spectrometer operated at 10 Torr with a radioactive ion source has been constructed and tested. The sensitivity of the instrument for typical VOCs such as acetone and isoprene can be several hundred Hz per ppbv. Its performance compares well with that of low pressure (1.5–2 Torr) proton transfer mass spectrometers; S_t on average scales with pressure as expected. At high pressure, care in the preparation of ions and maintenance of high E/N values (>120 Td) is important for maintaining high levels of H_3O^+ in the drift tube. This would be important for the detection of species that react at a significant rate with only the H_3O^+ species such as benzene and toluene [21].

Acknowledgements

Conversations with J. de Gouw, E.R. Lovejoy, C. Warneke, F. Eisele, T. Karl, A. Hansel, and W. Lindinger are gratefully acknowledged.

References

[1] W. Lindinger, A. Hansel, A. Jordan, Chem. Soc. Rev. 27 (1998) 347.
[2] A. Lagg, J. Taucher, A. Hansel, W. Lindinger, Int. J. Mass Spectrom. Ion Processes 134 (1994) 55.
[3] A. Hansel, et al., Int. J. Mass Spectrom. Ion Processes 149/150 (1995) 609.
[4] J. de Gouw, C. Howard, T. Custer, R. Fall, Geophys. Res. Lett. 26 (1999) 811.
[5] J.A. de Gouw, C.J. Howard, T. Custer, B.M. Baker, R. Fall, Environ. Sci. Technol. 34 (2000) 2640.
[6] R. Fall, T. Karl, A. Hansel, A. Jordan, W. Lindinger, J. Geophys. Res. 104 (1999) 15963.
[7] B. Noziere, C. Longfellow, B. Henry, D. Voisin, D. Hanson, Geophys. Res. Lett. 28 (2001) 1965.
[8] J. Williams, U. Pöschl, P. Crutzen, A. Hansel, R. Holzinger, C. Warneke, W. Lindinger, J. Lelieveld, J. Atmos. Chem. 38 (2001) 133;
T. Karl, R. Fall, P.J. Crutzen, A. Jordan, W. Lindinger, Geophys. Res. Lett. 28 (2001) 507;

C. Warneke, R. Holzinger, A. Hansel, W. Lindinger, J. Williams, U. Pöschl, P. Crutzen, J. Atmos. Chem. 38 (2001) 167.
[9] T. Karl, A. Guenther, A. Jordan, R. Fall, W. Lindinger, Atmos. Environ. 35 (2001) 491.
[10] L.G. Huey, E.J. Dunlea, E.R. Lovejoy, D.R. Hanson, R.B. Norton, F.C. Fehsenfeld, C.J. Howard, J. Geophys. Res. 103 (D3) (1998) 3355.
[11] J.A. Neuman, R.S. Gao, M.E. Schein, S.J. Ciciora, J.C. Holecek, T.L. Thompson, R.H. Winkler, R.J. McLaughlin, M.J. Northway, E.C. Richard, D.W. Fahey, Rev. Sci. Instrum. 71 (2000) 3886.
[12] R. Lapp, H. Andrews, Nuclear Radiation Physics, 3rd ed., Prentice-Hall, 1963, p. 115.
[13] I. Dotan, D. Albritton, W. Lindinger, M. Pahl, J. Chem. Phys. 65 (1976) 5028.
[14] C. Warneke, C. vander Veen, S. Luxembourg, J. de Gouw, A. Kok, Int. J. Mass Spectrom. Ion Processes 207 (2001) 167.
[15] G.H. Wannier, Bell Systems Tech. J. 32 (1953) 170.
[16] Y.K. Lau, S. Ikuta, P. Kebarle, J. Am. Chem. Soc. 104 (1982) 1462.
[17] A.J. Cunningham, J.D. Payzant, P. Kebarle, J. Am. Chem. Soc. 9 (1972) 7627.
[18] H. Ellis, M. Thackston, E. McDaniel, E. Mason, Atom. Nucl. Data Tables 31 (1984) 113.
[19] M. Meot-Ner, F.H. Field, J. Am. Chem. Soc. 99 (1977) 998.
[20] A. Hansel, W. Singer, A. Wisthaler, M. Schwarzmann, W. Lindinger, Int. J. Mass Spectrom. Ion Processes 167/168 (1997) 697.
[21] P. Spanel, D. Smith, Int. J. Mass Spectrom. Ion Process 181 (1999) 1.